

## **Effect of Particle Size Distribution on Processing and Properties of MIM 17-4PH**

Keith Murray, Andrew J Coleman, Toby A. Tingskog\* & Donald T. Whyhell Sr\*\*

Sandvik Osprey Ltd., Red Jacket Works, Milland Road, Neath, SA11 1NJ, U.K.

\*Sandvik Osprey Ltd., USA

\*\* CM Furnaces Inc, 103 Dewey Street, Bloomfield, N.J. 07003, USA

### **ABSTRACT**

17-4PH precipitation hardened stainless steel remains one of the most popular alloys used in Metal Injection Molding today. It is known that reported properties can vary significantly depending on chemistry, particle size and a host of processing variables that affect final density and phase structure. In this paper, we report the results of a systematic study of the effects of particle size distribution on sintering behavior and final properties of 17-4PH. Various size fractions (90%-10 $\mu$ m, 90%-16 $\mu$ m, 90%-22 $\mu$ m and -32 $\mu$ m) of gas atomized powder were extracted from the same parent batch and used for molding test samples. These were furnaceed at a range of temperatures to study the densification process and to determine the combined effects of particle size and sintering temperature on properties of interest. The relative merits of different size distributions are discussed in terms of sintering performance and distortion, tensile properties and surface finish.

### **INTRODUCTION**

Stainless steels continue to account for the majority of alloys used in MIM today and 17-4PH, along with 316L, is one of the most popular grades in use. 17-4PH exhibits an attractive combination of good sintering characteristics, high strength and good corrosion resistance at reasonable cost. It is also the authors' experience that there is increasing divergence in the range of particles sizes being used in MIM today. Not only are coarser grades, e.g. -32 $\mu$ m, becoming more popular but demand for finer grades, e.g. 90% -16 $\mu$ m and 90% -10 $\mu$ m, is also increasing for applications requiring superior detail and surface finish e.g. precision automotive and medical components.

It has been noted [1] that many applications are placing increasing demands on the mechanical properties that can be achieved with 17-4PH. A number of studies looking at the effect of processing conditions on the mechanical properties of 17-4PH have been published and a wide range of properties has been reported (e.g. see Fig. 1 below) in the as sintered and heat treated conditions: some values are well above MPlF35 typical values [1][2]. Post-sinter heat treatments, if employed, are in the range 480 – 590°C (H900 or H1100) and result in a significant boost in hardness and tensile strength. An intermediate solutionizing treatment at ~1050°C is sometimes employed.

The primary strengthening mechanism in these steels is by precipitation of coherent Cu particles. It has been speculated that variation in %Cu may be one of the reasons for differences in mechanical properties reported in the literature [3]. Increasing carbon content can also increase tensile strength: Mutterle et al. [4] reported %C to be inversely related to the quantity of  $\delta$ -ferrite in the microstructure, which causes a reduction in tensile strength. Gulsoy et al. [5] compared tensile properties of 17-4PH made from gas atomized and water atomized powders and found that H1050 properties of the gas atomized specimens were ~10% higher across a range of sintering temperatures (1250-1350°C). Kearns et al.[3] found, in a study of 15-5PH (sintering 1320-1380°C and 90%-22 to -38 $\mu$ m), that as-sintered tensile strength appeared to be little affected by particle size except at the lowest temperature studied where the coarsest powder (-38 $\mu$ m) showed a significantly lower strength level. The same trend was seen in the heat treated state (H1050) albeit the tensile strength was approximately 300MPa higher than 'as sintered'.

In this paper we report the results of a systematic study into the effects of both particle size distribution and sintering temperature on the densification behaviour and sintered properties of 17-4PH, extending the

range of powder size studied to finer sizes. The relative merits of different size distributions are also discussed in terms of sintering performance, part distortion, tensile properties and surface finish.

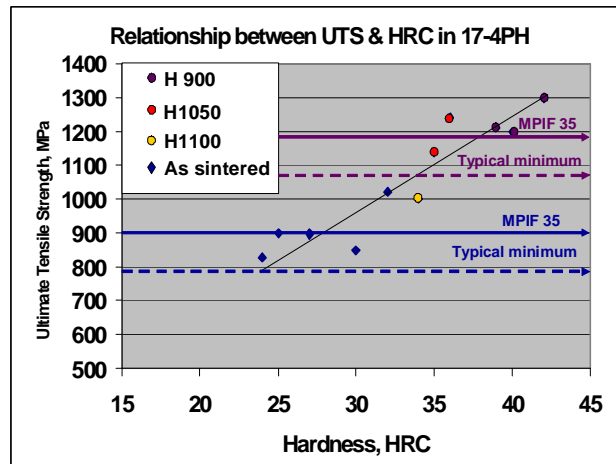


Fig 1: Selection of published mechanical property data for 17-4PH

## EXPERIMENTAL PROCEDURE

The 17-4PH powder used in this study was manufactured using proprietary gas atomisation technology. A single batch of powder was produced by induction melting the raw materials in an inert atmosphere and atomizing using nitrogen gas. The chemistry of the powder batch is shown in Table 1 and conforms to UNS S17400. From the as-atomized powder, four different size fractions were extracted by sieving and air classification, namely -32 $\mu$ m, 90% -22 $\mu$ m, 90% -16 $\mu$ m and 90% -10 $\mu$ m (see Fig. 2). Table 2 shows the particle size distribution and density data for these powders.

Table 1: 17-4PH chemical specification and powder analysis (as atomised powder)

Element	Specification (%)	Analysis (%)	Element	Specification (%)	Analysis (%)
Fe	Balance	Balance	Mn	1.00 max.	0.49
Cr	15.5 - 17.5	16.4	Si	1.00 max.	0.53
Ni	3.0 - 5.0	4.97	C	0.07 max.	0.037
Cu	3.0 - 5.0	4.29	P	0.04 max.	0.024
Nb	0.15 - 0.45	0.43	S	0.03 max.	0.001
O	-	0.062	N	-	0.078

Table 2: Particle Size Distribution data for evaluated powders (Malvern Mastersizer 2000)

Powder Size	D10 $\mu$ m	D50 $\mu$ m	D90 $\mu$ m	Tap Density $\text{gcm}^{-3}$	Apparent Density, $\text{gcm}^{-3}$	Density *(He pycnometer) $\text{gcm}^{-3}$
90% -10 $\mu$ m	3.25	5.82	10.00	4.03	3.04	5.227
90% -16 $\mu$ m	3.64	8.25	15.85	4.54	3.09	5.283
90% -22 $\mu$ m	4.58	11.05	21.76	4.47	3.35	5.335
- 32 $\mu$ m	4.33	12.17	27.71	4.80	3.55	5.302

\* measured by Advanced Metalworking Practices LLC

## Feedstock and Parts Manufacture

Four feedstock batches were compounded from the powders by Advanced Metalworking Practices LLC., of Carmel Indiana, using their proprietary multicomponent wax/polymer binder system. The feedstock had 6 weight % binder. The feedstocks were injection molded by NetShape Technologies Inc., of Solon Ohio, to produce MIMA standard tensile and Charpy test specimens.

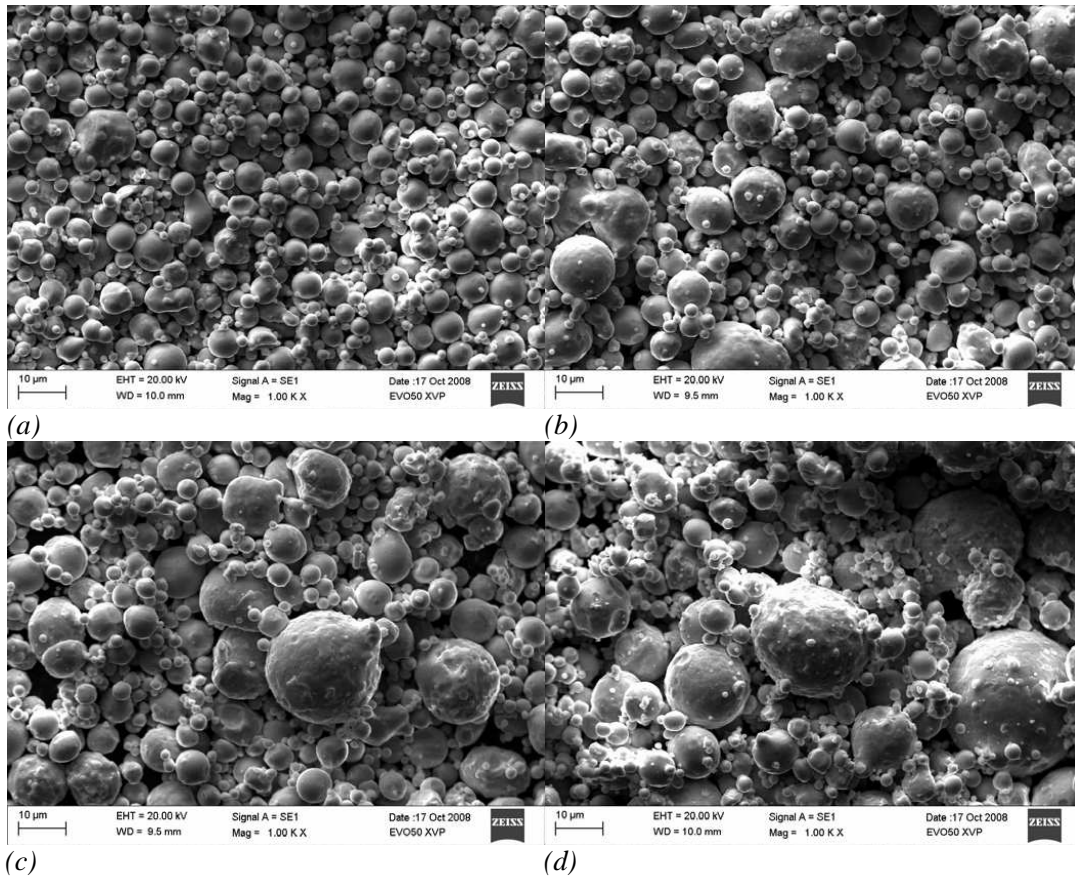


Fig 2: SEM images of (a) 90% -10µm, (b) 90% -16µm, (c) 90% -22µm and (d) -32µm powder

Sintering of the green parts manufactured from each of the four feedstock batches was carried out by CM Furnaces Inc., of Bloomfield, New Jersey, using a pusher furnace. The green parts were thermally dewaxed at 280°C (536°F) and sintered in a hydrogen atmosphere. Sintering was carried out in the range 1149°C to 1343°C (2100-2450°F) with a holding time at temperature of 2h and cooling rate of 10°C/min. As-sintered tensile samples were kept for triplicate testing and further samples were solutionized at 1038°C (1900°F) for 30min, water quenched and aged for 1h at 480°C (H900) followed by air cooling. Tensile testing was carried out on three specimens in each condition in accordance with ASTM E8-08. Vickers hardness testing was carried out using a 5kg weight. Sintered density measurements were carried out using the Archimedes method; porosity was measured by optical metallography and the level of  $\delta$ -ferrite formation was determined by phase analysis of microstructures etched in Kalling’s reagent. In order to evaluate distortion during sintering, Charpy test bars (2.5”x 0.5”x 0.25” green parts) were suspended across refractory supports, separated by 1.5” in the sintering furnace as shown in Figure 3a. After sintering the deflection of the Charpy bar was measured as shown in Figure 3b.

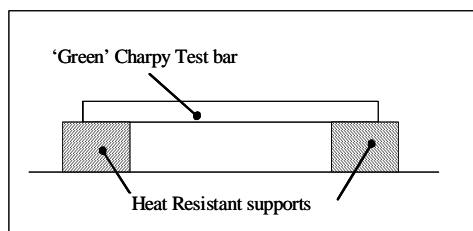


Fig 3a: Distortion test configuration

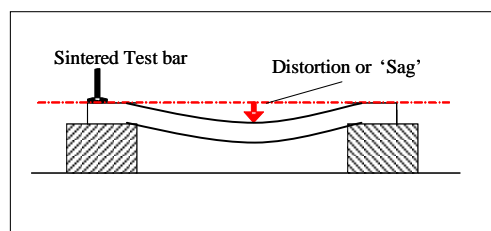


Fig 3b: Distortion measurement after sintering

## RESULTS

### Densification

After furnacing, metallographic analysis was carried out on sintered samples from each combination of particle size and sintering temperature. Images of the etched and polished microstructures obtained for the 90%-22 $\mu$ m particle size fraction across the range of sintering temperatures evaluated are contained in Fig. 4. Qualitative evaluation of the microstructures indicates that (1) grain size increases and (2) porosity decreases when the sintering temperature rises from 1149 - 1343 $^{\circ}$ C (2100-2450 $^{\circ}$ F).

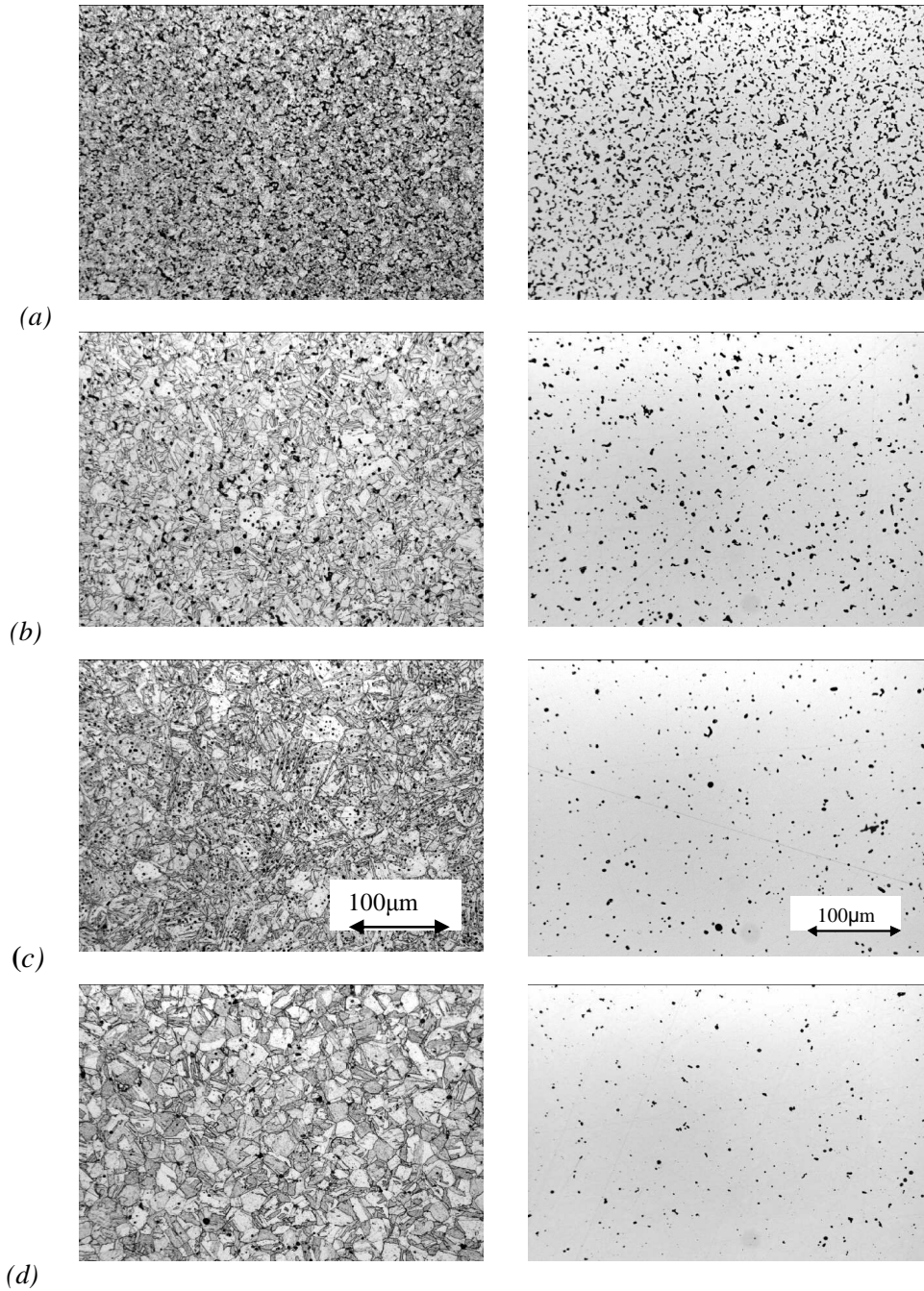
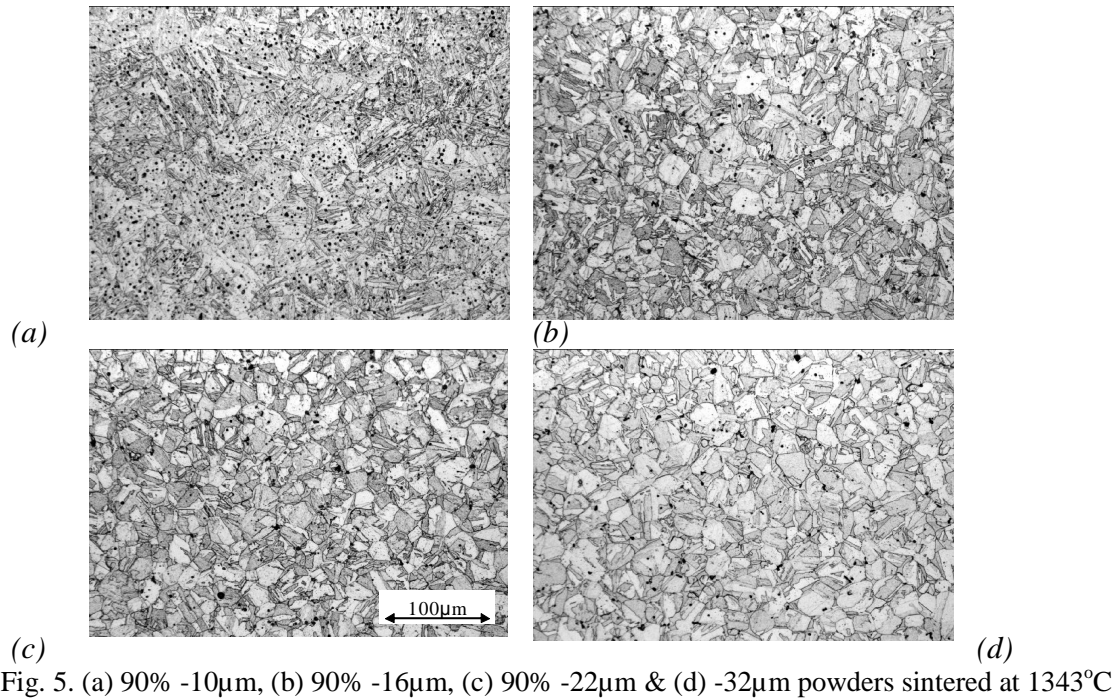


Fig 4: Etched and Polished microstructures of 'as sintered' 90% -22 $\mu$ m powder. Sintering temperatures (a) 1149 $^{\circ}$ C, (b) 1288 $^{\circ}$ C, (c) 1316 $^{\circ}$ C and (d) 1343 $^{\circ}$ C



Comparative metallographic analysis was also carried out on sintered samples produced from the four different particle size fractions processed at the same sintering temperature. Examination of the images in Fig. 5 indicates that there is a small increase in the as-sintered grain size with increasing powder size. The micrographs also show that the porosity level is highest for the 90%-10µm product, but is quite similar for the other three particle sizes. Quantitative analysis of sintered density was also carried out using the Archimedes method and results are shown in Fig. 6.

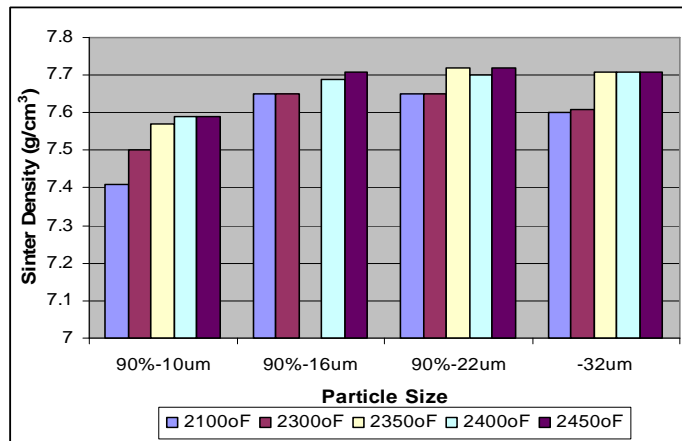


Fig 6: Density results for as sintered samples

The density results for the 90%-10µm samples are in the range 95.6 - 98% of theoretical and somewhat lower than the levels obtained for the other particle size ranges. Densities in excess of 98% of theoretical density were achieved across the full range of sintering temperatures for the other particle size ranges. Increasing the sintering temperature above 1288°C (2350°F) increased density levels beyond 7.7gcm<sup>-3</sup>, or 99% theoretical density.

Fig. 7 shows that the porosity in 90%-22 $\mu$ m samples drops dramatically from 1149°C (2100°F) and stabilizes at a low level above 1260°C (2300°F). It also shows the growth in the %  $\delta$ -ferrite above 1260°C (2300°F). Metallographic analysis shows that the  $\delta$ -ferrite phase is located primarily at the free surfaces of sintered samples.

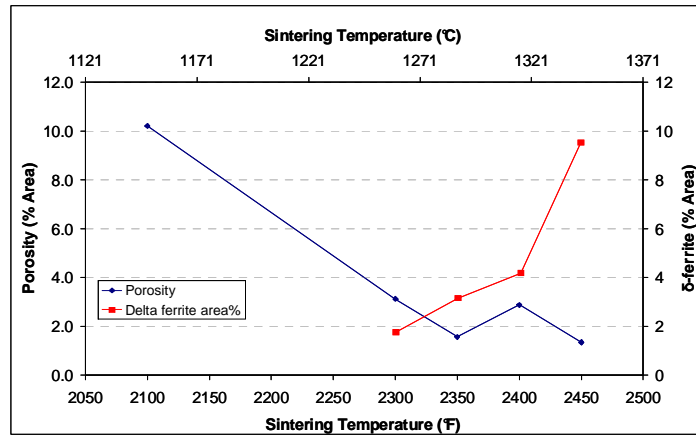


Fig 7: Porosity vs.  $\delta$ -ferrite of 90%-22 $\mu$ m powder as a function of sintering temperature

## Distortion

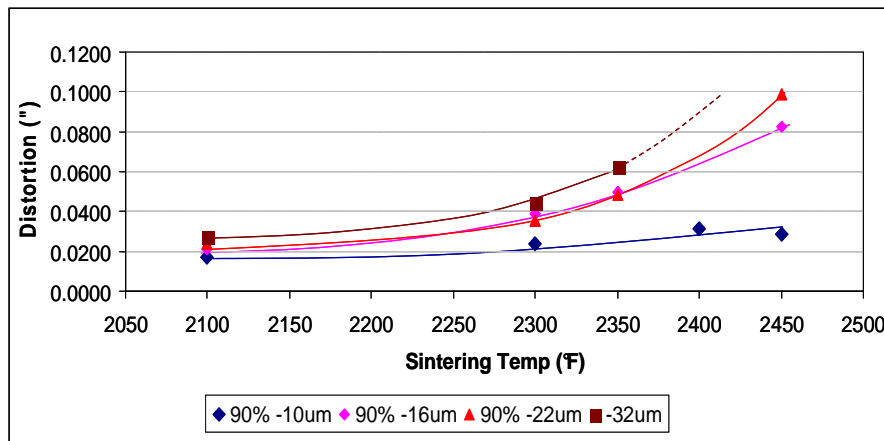


Fig 8: Relationship between distortion, powder size and sintering temperature

The data shown in Figure 8 indicates that, for a constant powder size, the level of part distortion increases with increasing sintering temperature. The data also show that the lowest level of distortion was observed on the 90% -10 $\mu$ m powder size samples across the full range of sintering temperatures.

## Mechanical Properties

Vickers Hardness data (5kg weight) have been converted to HRC in Figs 9 &10. ‘As sintered’ hardness values exceed the typical values outlined in MPIF Standard 35 for all powder sizes (Fig. 9) and there is little evidence of any effect of particle size on hardness. Fig.10, which is for 90% -22 $\mu$ m product, shows an initial rise in hardness with increasing temperature up to 1288°C (2350°F) above which there is a steady decline in hardness.

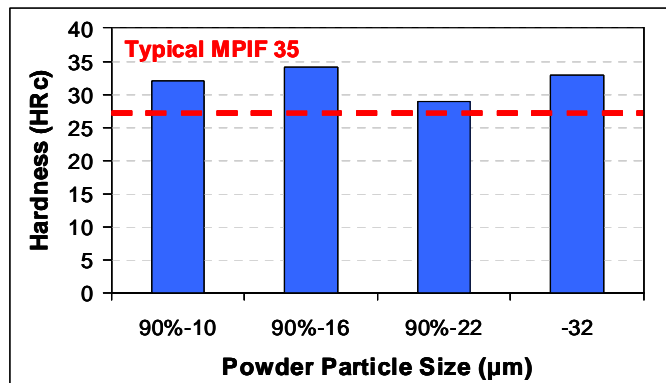


Fig. 9: Influence of particle size on 'as sintered' hardness of samples sintered at 1343 °C

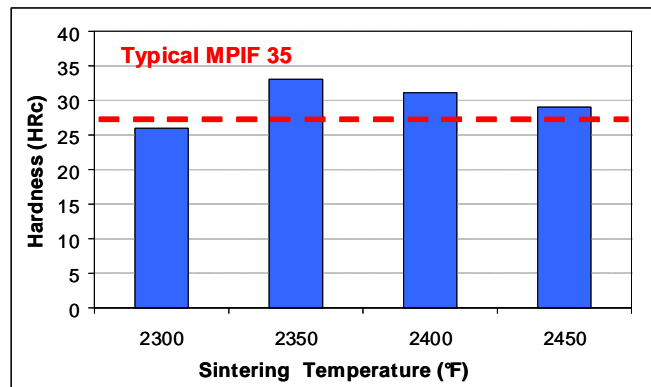


Fig 10: Influence of sintering temperature on 'as sintered' hardness of 90%-22µm samples

The tensile strength of both the 'as sintered' and heat treated samples increases as the sintering temperature increases from 1149 °C to 1288 °C, however no further benefit is seen at either 1316 °C or 1343 °C. The strength levels achieved at sintering temperatures at and above 1288 °C far exceed the typical MPIF Standard 35 values: indeed the peak values of 1485MPa (215ksi) are 300MPa higher than MPIF35 typical H900 values. At a sintering temperature of 1149 °C it would appear that there is an inverse relationship between tensile strength and particle size, such that decreasing particle size increases strength in both the 'as sintered' and heat treated conditions. As the sintering temperature

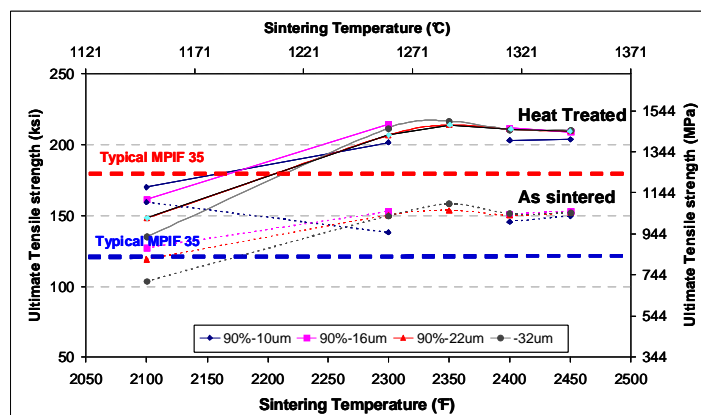


Fig 11: Influence of particle size and sintering temperature on 'as sintered' & H900 UTS

increases, the influence of particle size on tensile strength diminishes such that at temperatures of 1288 °C (2350 °F) and above tensile strength appears to be independent of particle size. In the case of the 90% -10µm powder sintered at 1149 °C (2100 °F), however, the measured tensile strength in the ‘as sintered’ condition is significantly higher than the values obtained for the other powder sizes. Chemical analysis of the sample indicates that the carbon level is below 0.01%, which is significantly lower than the level of 0.037% measured for the bulk material.

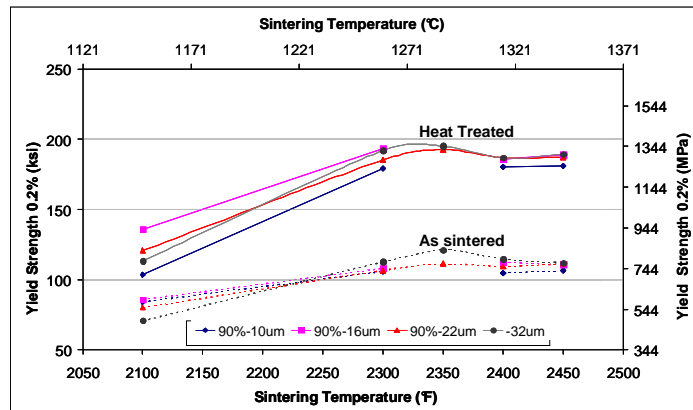


Fig 12: Influence of particle size and sintering temperature on ‘as sintered’ & H900 0.2% YS

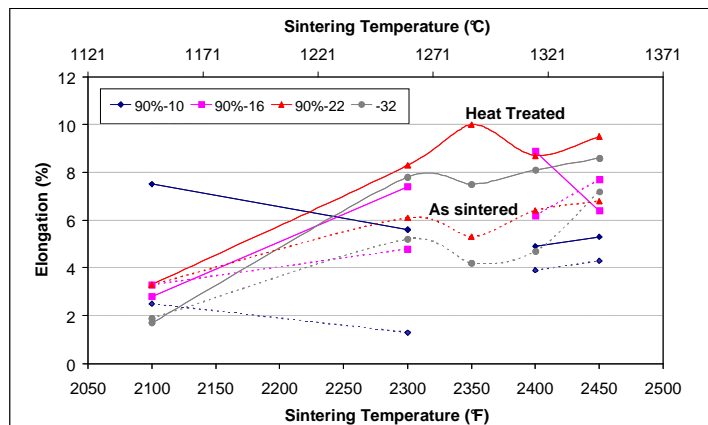


Fig 13: Influence of particle size and sintering temperature on elongation of ‘as sintered’ & H900

Figs 12 & 13 show the progression in yield strength and ductility of 17-4PH in the as sintered and H900 condition with increasing sintering temperature. The yield strength shows plateau values above 1260°C (2300°F) and the ductility values (with the exception of 90%-10µm) are all > 4% for as sintered specimens and > 6% for H900 heat treated specimens at sintering temperatures ≥ 1260°C.

## DISCUSSION

The powder size distributions chosen for this study cover the most popular size ranges chosen for the PH family of stainless steels. Finer powder fractions are used for special applications requiring precise dimensional control, thin-walled components and/or excellent surface finish where superior moulding characteristics are essential. The coarser sizes examined here are relatively low cost alternatives and it is

therefore worthy of investigation whether acceptable properties can be achieved in order to extend the range of applications where MIM'ed 17-4PH can offer a cost effective solution.

The powder size data listed in Table 2 show clear relationships with both apparent and tap density: fine powders show lower density due to higher inter-particle friction and inferior particle packing. The relatively low pycnometric density values for the smaller particle size fractions may reflect the higher proportion of surface oxide and nitride that would be expected in these fractions. The use of a fixed powder loading with 6 wt% binder in this study therefore means that the inter-particle spacing will be smaller for the finer powders and this is reflected in the lower distortion shown in Fig. 8 for finer powders as the sintering temperature increases. These results may be compared with those of Bulger et al. [6] who demonstrated that distortion of 17-4PH parts decreases with increased powder loading.

Compared with earlier studies that show peak strength is achieved at temperatures approaching 1350°C (2462°F), the present results show that for all powder sizes, a plateau in strength levels and ductility begins at ~1288°C (2350°F) and is maintained up to 1343°C (2450°F). This corresponds to a threshold temperature above which >98% theoretical density is achieved. It is also apparent that above this temperature, an increasing proportion of  $\delta$ -ferrite is observed in the microstructure and this agrees with earlier observations by Gulsoy et al. [5]. While  $\delta$ -ferrite promotes more complete sintering, it has a deleterious effect on tensile properties which may help explain the small decline in strength >1300°C (2372°F). The appearance of  $\delta$ -ferrite in hydrogen sintered PH stainless steels has been commented upon previously by Blaine et al. [7] who determined that  $\delta$ -ferrite is enhanced in pure hydrogen compared with nitrogen/hydrogen atmospheres where nitrogen tends to stabilize austenite which retards diffusion and densification.

Regarding the impact of particle size distribution on mechanical properties, it is surprising that the 90%-10 $\mu$ m powder displays the lowest sintered density despite evidence elsewhere that as powders become finer, sintering activity increases and full density can be achieved at lower temperatures. Imbaby et al [8] for example report that 99% density is obtained from 90%-4 $\mu$ m 316L powder at 1200°C (2192°F). The reasons for the anomalous behavior of the 90%-10 $\mu$ m powder are unclear, but it may be that after early fast densification, fine porosity is trapped in the bulk. In support of this, it was apparent that  $\delta$ -ferrite is more prevalent at the free surfaces of the sintered samples. Complementary dilatometric studies on the different powders suggest that with sufficiently slow heating rates, the 90%-10 $\mu$ m powder does indeed begin sintering earlier than coarser powders and that it achieves high density [9]. Aside from the 90%-10 $\mu$ m powder, it appears that there is little to choose among the finest to the coarsest products in terms of mechanical properties albeit the highest sintering temperature is needed for the coarsest powder in order to achieve best strength levels. Therefore, there appears to be freedom to choose powder size depending on moldability, part precision, surface finish and cost.

## SUMMARY & CONCLUSIONS

Gas atomized 17-4PH powders in the range 90%-10 $\mu$ m to -32 $\mu$ m have been molded to examine effects of particle size and sintering temperature on tensile properties. Tensile strength increases with increasing sintering temperature up to 1288°C with peak values 1130MPa 'as sintered' and 1490MPa 'H900'. These strength levels are well above values reported elsewhere. In the as-sintered state, there appears to be little effect of particle size distribution on tensile strength except for lowest temperature sintering and finest powder, where significantly lower strength levels are achieved. The same trend is seen in the heat treated state where tensile strength in general is approximately 350MPa higher. Therefore, equivalent strength level can be achieved with coarser powders provided the sintering temperature is raised sufficiently.

Sintering begins earlier with finer powders leading to lower distortions at any given temperature. However, in this work, the 90%-10 $\mu$ m powder gave a surprisingly low finished density which is suspected to be due to trapping of finely dispersed porosity in the microstructure.

## **ACKNOWLEDGEMENTS**

Thanks are due to Matt Bulger and colleagues at NetShape Technologies for molding the tensile and Charpy specimens used in this study and to Linn Larsson of Sandvik Materials Technology, Sandviken, for coordinating hardness testing and metallographic studies.

## **REFERENCES**

1. T. McCabe, 'Materials Design: Advanced Stainless Steels through PIM Processing', MIM2010, Long Beach California 2010
2. R. German, 'Designing for MIM: a Guide for Designers and End-users', PIM International, Vol 2, No.4 December 2008.
3. M.A.Kearns et al, 'Effects of Particle Size and Alloy Chemistry on Processing and Properties of MIM Powders', Powdermet 2009, Las Vegas, Nevada 2009
4. P.V.Muterlle et al., 'Influence of Carbon Content on Microstructure and Tensile Properties of 17-4PH Stainless Steel produced by MIM', PIM International, Vol 2, No.4 December 2008.
5. H.O.Gulsoy, S. Ozbek & T. Baykara, Microstructural & Mechanical Properties of Injection Moulded Gas and Water Atomised 17-4PH Stainless Steel Powder. Powder Metallurgy Vol 50(2) 2007 120-126.
6. M. Bulger, 'The Relationship between Feedstocks Loading and Component Distortion in a Production MIM Process, MIM2010, Long Beach California 2010
7. M. Imbaby & K. Jiang, 'Fabrication Process of 3D Micro Components from Stainless Steel Aqueous Slurry', Proc. World Congress on Engineering 2009 Vol 1, WCE 2009, July 2009, London.
8. D.C Blaine et al., 'Sintering Shrinkage and Microstructure Evolution during Densification of a Martensitic Stainless Steel, 2003.
9. M.A.Kearns, T.Tingskog & J.Strauss, 'Dilatometric Studies on 17-4PH at Different Particle Size Ranges'. To be published.